STM JOURNALS

Journal of
Polymer & Composites

https://journals.stmjournals.com/jopc

ISSN: 2321-2810 (Online)
ISSN: 2321-8525 (Print)
Volume 14, Issue 4, 2026
DOI (Journal): 10.37591/JoPC

Research JoPC

Low-Weight, High-Durability Crankshaft Development Using Glass Fiber Composites: Numerical and Experimental Investigations

Sandeep S Sarnobat[1], Sandeep M Shiyekar[2,*], Kiran Choudhary[3]

Abstract

The present paper aims towards the weight reduction of crankshaft by replacing conventional medium carbon steel for a two-wheeler with composite material. The replacement is such that it significantly reduces load on other components without compromising structural integrity. It will also serves in terms of operating reliability or durability over its life span. A geometric specifications and dimensions were obtained using a 3D CAD model developed in CATIA V5. The model was later imported to HyperMesh, where the mesh generation process took place correspondently achieving high quality discretization for finite element analysis. ANSYS APDL was then used to perform static structural and fatigue analyses of the crankshafts made from steel, glass fiber composite, and carbon fibre composite considering realistic service loading conditions The comparative analysis shows that the crankshaft made of glass fiber composite has better performance. The performance was compared with the normal steel crankshaft and von Mises stress were decreased by 26.99%, and a better load-carrying capacity is obtained owing to good macroscopic distribution of loads on it. Additionally, 16.66% fatigue life improvement for the glass fiber configuration indicates higher resistance to cyclic loading and longer service-life. Most notably, a substantial weight reduction of 75.88% was achieved, highlighting the potential of glass fiber composites as a high-performance, lightweight alternative for crankshaft applications. There is an improvement in terms of fuel efficiency, inertial forces affecting performance and emissions. These results indicate a great scope for utilizing glass fiber composites material system in future two-wheeler crankshaft applications.

Keywords: Crankshaft, composite materials, structural integrity, stress analysis, deformation, fatigue life

***Author for Correspondence**
Sandeep M Shiyekar
E-mail: smshiyekar@dypcoeakurdi.ac.in

[1]Professor, Department of Robotics and Automation, D Y College of Engineering Akurdi, Pune, India; Savitribai Phule Pune University, Pune, Maharashtra, India
[2]Professor, Department of Civil Engineering, D Y College of Engineering Akurdi, Pune, India; Savitribai Phule Pune University, Pune, Maharashtra, India
[3]Research Scholar, Department of Robotics and Automation, D Y College of Engineering Akurdi, Pune, India; Savitribai Phule Pune University, Pune, Maharashtra, India

Received Date: May 22, 2026
Accepted Date: June 05, 2026
Published Date: July 08, 2026

Citation: Sandeep S Sarnobat, Sandeep M Shiyekar, Kiran Choudhary. Low-Weight, High-Durability Crankshaft Development Using Glass Fiber Composites: Numerical and Experimental Investigations. Journal of Polymer & Composites. 2026; 14 (4): 310–325p.

INTRODUCTION

The crankshaft is a fundamental mechanical component responsible for transforming the reciprocating motion of the piston into the rotational motion required to drive the engine. It consists of crankpins whose axes are offset from the main crank axis, enabling the conversion of linear piston motion into circular rotation. The crankshaft is connected to a flywheel, which stabilizes engine speed by reducing torsional vibrations and acting as a vibrational damper. Because of its continuous exposure to cyclic bending and torsional loads, the crankshaft must be designed for high reliability and fatigue resistance.

Crankshafts have been numerically studied in the past by means of finite element analysis (FEA) computational techniques for purpose of determining its structural, fatigue and failure behaviour. Suganthini et al. [1] studied modelling and analysis of crankshafts with metal matrix composites for improved strength-to-weight characteristics. FEA was used by Pore and Kotkar [2] on aluminium alloy crankshafts for optimization of weight. Gopal et al. [3] studied the behaviour of piston, connecting rod and crankshaft assemblage during dynamic conditions.

Witek et al. [4–5] investigated stress, fracture and fatigue on diesel engine crankshafts discovered aspect between fillet regions where fatigue crack at initiation occurred. Jamalkhani and Azadi [6] studied criterion for evaluating the High-Cycle Fatigue Behaviour of Shaft Structures made of ductile cast iron. Zhenpeng et al. [7] studied NVH and reliability characteristics with crankshaft-bearing interaction models.

Satishkumar and Kannan [8] conducted thermo-mechanical modelling of engine pistons by CAE tools. Fonte et al. [9] conducted an analysis of failure modes on diesel engine crankshafts and fatigue was determined to be the root cause. Senthilkumar et al. [10] studied the failure of crankpins caused by stress concentration and lubrication.

Bagde and Raut [11] performed finite element modelling (FEM) on fatigue analysis of single cylinder engine crankshaft using ANSYS. Thejasree et al. [12] modelled the crankshaft in FEM under operational loads. Theoretical investigation of crack propagation and failure behaviour using FEA approaches was carried out by Kahate and Keche [13].

Patil and Pawar [14] studied on ANSYS software of composite crankshafts. Mathapati and Dhamejani [15] and Devara AK [16] used FEM for evaluation of stresses and deformations in Crankshaft Systems.

Kolhe et al. [17] used FEA-based methods for the estimation of the fatigue life of diesel engine crankshafts. Ramani et al. [18] performed FE-analysis and sought measures to improve breathing capacity and structural activation of IC engine crankshafts. Kakade and Pasarkar [19] summarized the causes of crankshaft failures such as fatigue loading and stress concentration effects.

Kumbhar et al. [20] conducted design and failure study of six-cylinder diesel engine crankshafts against operational stresses. These methodologies are based on finite element-based crankshaft failure analysis. The importance of fatigue evaluation has been discussed by Naik [21]. Fatigue behaviour of automotive crankshafts under operating load spectra and evaluation of the effect of cyclic load fluctuations on fatigue life prediction was performed by Marpudi and Mehra [22].

To enhance the efficiency of composite materials, recent research has mainly focused on using recycled and natural resources for sustainable composite systems. The incorporation of recycled waste manhole covers and fibreboard residues into thermoplastic composites as reinforcing fillers led to improved mechanical properties, besides enabling the valorisation of waste [23]. Subsequent studies on Grewia monticola fibres confirmed their potential as bio sustainable reinforcements due to their desirable physical, thermal, and mechanical properties [24]. In more wider applications of natural fibres, the enhancement in strength and stiffness was very much significant from 200 MPa to 1570 MPa of Phormium Tenax reinforced natural rubber composites [25]. In the same way, its hybrid epoxy composites reinforced with Areca catechu fibres and silicon carbide particles yielded improved mechanical and wear performance [26]. Additionally, alkali treatment of Acacia caesia bark fibres has enhanced fibre surface characteristics, tensile properties and interfibrillar bonding within the fibre-matrix interface leading to effective reinforcement for bio-composites [27]. The above studies emphasize the potential use of natural fibres, recycled materials and hybrid reinforcements in sustainable high performance composite systems.

Journal of Polymer & Composites
Volume 14, Issue 4
ISSN: 2321-2810 (Online), ISSN: 2321-8525 (Print)

In contemporary automotive engineering, reducing the weight of rotating components such as crankshafts has become increasingly important for improving fuel efficiency, enhancing engine responsiveness, and reducing emissions. Weight optimization is typically achieved through two approaches: topology optimization, which modifies geometry to minimize unnecessary mass, and material optimization, which replaces existing materials with lighter alternatives while maintaining mechanical integrity. This study adopts material optimization and investigates the feasibility of using glass fiber as a replacement for steel in crankshaft applications. Glass fiber, with a density of approximately 1.9 g/cm^3, offers the potential for 60–70% weight reduction while still delivering mechanical properties comparable to many metallic alloys.

Composite materials achieve tailored structural performance by combining reinforcement fibers with a polymer matrix. Unlike metals, which are isotropic and exhibit uniform properties in all directions, fiber-reinforced composites are inherently anisotropic, exhibiting significantly higher stiffness and strength along the fiber direction. The matrix binds the fibers, transfers load between them, maintains their orientation, and provides environmental protection and thermal stability. Through appropriate fiber orientation and stacking sequences, composite components can be engineered to achieve desirable stiffness, strength, and fatigue resistance.

In two-wheeler engines, crankshafts are commonly manufactured from medium carbon steel, which provides an effective balance of stiffness, durability, and manufacturability. However, in the current landscape of advanced automotive design, the demand for lighter components continues to increase, motivating the exploration of composite alternatives. Glass fiber and carbon fiber have emerged as promising options due to their superior strength-to-weight ratios and customizability. Glass fiber offers excellent fatigue resistance and moderate stiffness at a significantly lower density than steel, while carbon fiber provides high stiffness but may not always satisfy dimensional stability requirements under combined bending and torsional loads.

In the present study, finite element analysis (FEA) is employed to evaluate the structural and fatigue performance of glass fiber and carbon fiber crankshafts as replacements for steel. A three-dimensional CAD model of the crankshaft is developed, and stress, deformation, and fatigue life are calculated for each material configuration. To validate the numerical predictions, experimental fatigue testing is performed on an optimized crankshaft prototype. This integrated approach demonstrates how advanced material engineering combined with computational fatigue modelling can pave the way for lighter, more efficient engine components.

Fatigue Theory

Strain-Life (ε–N) Method

The strain-life method is particularly suited for low-cycle fatigue, where localized plastic deformation plays a significant role in crack initiation. Total strain amplitude is expressed using the Coffin–Manson–Basquin relation:

$$\varepsilon_a = \frac{\sigma_f'}{E}(2N_f)^b + \varepsilon_f'(2N_f)^c \tag{1}$$

where

σ_f'= fatigue strength coefficient, ε_f'= fatigue ductility coefficient, b= fatigue strength exponent, c= fatigue ductility exponent, E= Young’s modulus, N_f= cycles to failure.

This method captures elastic–plastic strain behavior at stress concentration regions and predicts fatigue crack initiation life.

Stress-Life (S–N) Approach

For high-cycle fatigue, where deformation remains almost entirely elastic, the stress-life method is used. The Basquin relationship:

$$\sigma_a = \sigma_f'(2N_f)^b \quad (2)$$

defines the stress amplitude corresponding to the number of cycles to failure. S–N curves characterize fatigue behavior over millions of cycles and are widely applied for metals under high-cycle fatigue conditions. This approach predicts total fatigue life, accounting for both crack initiation and propagation in elastic-dominated regimes.

Fracture Mechanics

Fracture mechanics offers a more complete representation of fatigue by focusing on crack propagation. The Paris law quantifies crack growth per cycle:

$$\frac{da}{dN} = C(\Delta K)^m \quad (3)$$

where crack growth rate depends on the stress intensity range ΔK. Total fatigue life is therefore expressed as:

$$Life = Initiation + Propagation$$

This method is essential for components where cracks already exist or initiation life is negligible compared to propagation life.

Ansys Workbench Fatigue Methodology

Fatigue analysis in ANSYS Workbench begins with establishing a robust finite element model that accurately represents the geometry and stress distribution of the crankshaft. Once the mesh and boundary conditions are defined, static or transient analyses provide stress and strain fields that form the foundation for fatigue evaluation. The fatigue module then incorporates material-specific fatigue properties—either in strain-life or stress-life form—and superimposes constant or variable amplitude load histories on the FEA stress field.

To account for localized plasticity, ANSYS applies Neuber's hyperbolic rule, which corrects for the mismatch between linear elastic FEA predictions and actual elastic–plastic material response. Adjustments for mean stress are made using theoretical models before querying the appropriate S–N or ε–N curves. ANSYS also reduces multiaxial stress states to equivalent uniaxial values using signed von Mises stress or principal stress transformations. Under variable-amplitude loading, rainflow cycle counting decomposes the load-time history into closed stress cycles, each evaluated independently. Miner's cumulative damage rule then accumulates the contribution of each cycle, facilitating an overall fatigue life prediction.

The software ultimately presents fatigue life, fatigue damage, and factor of safety contours, providing detailed insight into the structural integrity and durability of critical regions of the crankshaft.

Loading Types in ANSYS

Fatigue loading conditions govern how damage accumulates over time, and ANSYS categorizes loading into proportional and non-proportional scenarios. In proportional constant-amplitude loading, all stress components scale together, and principal stress directions remain fixed. This permits fatigue life estimation from a single FEA stress state. Conversely, non-proportional loading arises when principal stress directions rotate, as seen in components subjected to combined bending and torsion; such cases require multiple load states for accurate assessment.

Variable-amplitude loading reflects real-world operating environments, such as fluctuating combustion pressure or road-induced vibrations. When these loads are proportional, fatigue cycles can still be derived from a single stress pattern. However, variable-amplitude non-proportional loads generate complex multiaxial stress paths that challenge fatigue modelling accuracy. ANSYS addresses this complexity through rainflow counting and advanced multiaxial reduction methods, enabling realistic fatigue analysis across diverse operating scenarios.

Mean Stress Corrections

Mean stress has a profound effect on fatigue behavior. Since most fatigue data assumes fully reversed loading, mean stress corrections ensure accuracy under real service conditions. The Goodman relation provides a simple, conservative linear correction ideal for brittle materials. The Gerber parabola yields a more accurate nonlinear correction for ductile metals. The Soderberg model is the most conservative, restricting allowable stress based on the yield strength.

Goodman: $\frac{\sigma_a}{S_e} + \frac{\sigma_m}{S_u} = 1$ (4)

Gerber: $\frac{\sigma_a}{S_e} + (\frac{\sigma_m}{S_u})^2 = 1$ (5)

Soderberg: $\frac{\sigma_a}{S_e} + \frac{\sigma_m}{S_y} = 1$ (6)

For strain-life applications, Morrow's method modifies elastic strain amplitude to reflect mean stress effects, while the Smith–Watson–Topper (SWT) parameter integrates maximum stress and cyclic strain:

$$P_{SWT} = \sigma_{max}\, \varepsilon_a \quad (7)$$

These corrections improve the reliability of fatigue predictions across a wide range of loading conditions.

Multiaxial Stress Processing in Fatigue Analysis

Mechanical components such as crankshafts rarely experience uniaxial loading; instead, they endure complex combinations of bending, torsion, and axial forces. ANSYS simplifies these conditions by converting multiaxial states into equivalent uniaxial fatigue parameters using von Mises or principal stress transformations. Signed von Mises stress is particularly useful, as it preserves the sign of the stress state, enabling appropriate application of mean stress corrections.

von Mises: $\sigma_{vm} = \sqrt{\frac{(\sigma_1-\sigma_2)^2+(\sigma_2-\sigma_3)^2+(\sigma_3-\sigma_1)^2}{2}}$ (8)

Signed von Mises: $\sigma_{vm}^{signed} = sign(\sigma_1)\, \sigma_{vm}$ (9)

Fatigue Modifiers

Real-world conditions rarely match laboratory test environments. Variations in surface finish, size effects, environmental exposure, and reliability requirements influence fatigue behavior. ANSYS accounts for these influences through fatigue strength modifiers, load scaling factors, and interpolation schemes for fatigue curves. These modifiers collectively refine fatigue predictions, making them more reflective of industrial conditions.

Fatigue Results, Hysteresis, Rainflow, and Damage Matrix

ANSYS outputs fatigue life and fatigue damage maps that highlight regions susceptible to early failure. In strain-life analysis, hysteresis loops illustrate energy dissipation per cycle, indicating localized plastic deformation. Rainflow cycle counting extracts closed cycles from variable-load histories, providing the basis for fatigue calculations. Miner's rule accumulates damage indices from individual cycles:

$$D = \sum \frac{n_i}{N_i} \quad (10)$$

A damage matrix visually captures how cycles are distributed across combinations of mean and alternating stress, offering deeper insight into fatigue behavior.

METHODOLOGY

The methodology adopted in the present investigation follows a structured and scientifically grounded sequence, beginning with analytical evaluations of crankshaft geometry and loading, and progressing toward finite element modelling and fatigue assessment. These preparatory analytical calculations form the foundation for the numerical investigation and ensure that the finite element analysis (FEA) reflects realistic engine operating conditions.

Table 1. Crankshaft Geometry.

Symbol	Parameter	Value
D	Piston Diameter	52.4 mm
lc	Length of Crankpin	56 mm
dc	Diameter of Crankpin	28 mm
L	Stroke	57.9 mm
ds	Shaft Diameter	22 mm
t	Thickness of Crank Web	28 mm
w	Width of Crank Web	28 mm
r	Shaft Center to Web Center	37 mm

The geometric parameters and derived quantities for the crankshaft, summarized in Table 1, were used as essential inputs for the FEA model. These dimensions not only define the structural configuration of the crankshaft but also play a decisive role in determining its stress distribution, deformation characteristics, and fatigue response.

Determination of Combustion Load

To accurately determine the mechanical load acting on the crankpin during the power stroke, the thermodynamic properties of petrol combustion were employed. The density of petrol ($\boldsymbol{\rho}$) was considered as 719.7 kg/m^3, and the operating temperature (T) during combustion was taken as 573 K. Based on the swept volume of the cylinder, the mass of trapped charge was calculated as:

$$m = \rho \times V = 0.0898\, kg$$

The molecular mass of petrol was assumed to be $M = 136.238 \times 10^{-3}$kg/mol, and the universal gas constant $R = 8.314472\, J\, mol^{-1}\, K^{-1}$.

Applying the ideal gas relation,

$$PV = nRT, \tag{11}$$

where

$\boldsymbol{P}$= in-cylinder pressure during the power stroke, $\boldsymbol{V}$= combustion chamber volume, $\boldsymbol{n} = \frac{\boldsymbol{m}}{\boldsymbol{M}}$= number of moles of fuel–air mixture,

substituting the corresponding values yields:

$$P \times 124.9 = 0.0898 \times 8.314 \times 573P = 3.425\, MPa$$

This represents the peak pressure exerted on the piston crown during combustion.

Evaluation of Gas Force Acting on The Crankpin

The force exerted on the piston due to combustion pressure (gas force, $\boldsymbol{F_p}$) is calculated using:

$$\boldsymbol{F_p} = \boldsymbol{P} \times \boldsymbol{A} \tag{12}$$

Where

$P = 3.425\, MPa$ is the combustion pressure, $A = \frac{\pi D^2}{4}$ is the piston crown area.

Substituting the piston diameter $\boldsymbol{D} = \mathbf{52.4}$mm:

$$F_p = 3.425 \times \frac{\pi}{4}(52.4)^2$$

$$F_p = 7202.75\, N \approx 7.2\, kN$$

Journal of Polymer & Composites
Volume 14, Issue 4
ISSN: 2321-2810 (Online), ISSN: 2321-8525 (Print)

Table 2. Comparison of material properties.

Property	Steel	Carbon fiber	Glass fiber
Young's Modulus, (E) (MPa)	210000	126900	40300
Poisson's Ratio, (ν)	0.30	0.20	0.20
Density, (ρ) (kg/m³)	7850	1600	1900
Shear Modulus (MPa)	80000	6600	3070

Table 3. Comparative performance of crankshaft materials.

Material	Deformation (mm)	von Mises stress (MPa)	Fatigue life (cycles)	Weight reduction (%)
Steel	0.01	55.39	1,000,000	Baseline
Carbon Fiber	0.17	67.99	991,000	67.45
Glass Fiber	0.16	40.44	1,200,000	75.88

This gas force is transmitted through the connecting rod and acts directly on the crankpin. Therefore, $\boldsymbol{F_p}$ represents the critical load applied in the finite element model and serves as the primary boundary condition for evaluating crankshaft stresses, deformation profiles, and fatigue behavior under peak operating conditions.

Material Properties

To evaluate and optimize the structural performance of the crankshaft, three candidate materials were selected for investigation: the conventional 42CrMo4 steel used in automotive crankshafts, and two widely used composite alternatives carbon fiber and glass fiber. Prior to conducting numerical simulations, a comparative assessment of their fundamental mechanical properties was carried out to establish a clear basis for material selection and experimental design. The material comparison, summarized in Table 2, highlights key properties such as Young's modulus, Poisson's ratio, density, and shear modulus, all of which directly influence stiffness, mass reduction potential, and overall fatigue performance of the crankshaft.

The strength of composites may be highly anisotropic–that is, it varies with the direction of the applied load (normal and shear). The load is applied in the direction parallel to the fibre axis (0^0) and the maximum tensile strength can be attained, since high-modulus fibers carry most of stress. In contrast, transverse loading (90^0) depends on the much weaker polymer matrix that fails prematurely in crack propagation. Intermediate angles admit additional types of shear stress and coupled deformations (e.g. bend-twist coupling). Using a "stacking sequence" of plies at different angles (e.g., [0/±45^0/90^0]s), engineers can customize the laminate to follow a certain flow of loads, so that the product is much more structurally efficient than isotropic metals.

Getting past black aluminium design, which treats composites as isotropic materials is needed to replace metals. Designers must apply Classical Laminate Theory (CPT) with certain ply orientations (0^0,±45^0,90^0) (i. Stress concentrations at holes or sharp corners are very critical, as composites have little or no plastic deformation of metals. Therefore, large radii and the use of special inserts for mechanical joints is required. Internal stresses at interfaces related to different Coefficient of Thermal Expansion (CTE) must be managed. Lastly, the electrical conductivity of carbon fibre can also create galvanic corrosion when in contact with aluminium that requires fiberglass isolation layers or titanium fasteners.

Composites fail via multiple mechanisms simultaneously that are very difficult to unpick (e.g. Fiber breakage, matrix cracking and delamination). 'Grip effects', where the very high clamping pressure needed to avoid slipping, either crushes the specimen or results in invalid failures at the ends, impedes standard testing. To remedy this, bonded end tabs should be used for redistribution of loads into the gauge section of specimens. Another challenge lies in environmental sensitivity, as the polymer matrix can absorb moisture and soften under heat (necessitating "hotwet" conditioning to mimic long-term degradation). Lastly, expensive nondestructive testing (NDT) such as ultrasonic C-scans are required to confirm structural integrity since the internal damage itself is typically invisible around-the-eye.

Development of the 3d Cad Model of the Crankshaft

The creation of an accurate and fully detailed three-dimensional CAD model forms the foundation of the crankshaft optimization process. Because the crankshaft experiences complex interactions of bending, torsion, and axial forces during engine operation, the geometric fidelity of the model is critical for obtaining reliable simulation results. A precisely defined CAD model ensures that key structural features—such as fillets, crankpins, journals, counterweights, and web thicknesses—are represented with the level of detail necessary to capture stress concentrations and dynamic behaviour under cyclic loading.

The 3D CAD model was developed using industry-standard modelling software, adhering strictly to the geometric dimensions derived from analytical calculations and design specifications. Figure 1 illustrates the dimensional characteristics of the crankshaft, serving as the reference configuration for subsequent analyses. This geometric blueprint provides the structural scaffold for performing material substitution studies, evaluating mechanical responses, and ensuring simulation accuracy throughout the optimization workflow.

The CAD model not only defines the physical shape of the crankshaft but also directly influences mesh quality, boundary condition application, and the accuracy of stress distribution predictions in the finite element model. Thus, its development represents a crucial early-stage step, enabling all downstream stages of structural assessment, material comparison, and fatigue evaluation to be conducted with precision.

Finite Element Analysis (FEA)

A high-fidelity finite element model is essential for accurately predicting the structural behavior of the crankshaft under operational loads. To achieve this, a detailed meshing strategy was implemented within ANSYS Workbench, executed on a high-performance system equipped with an Intel i7 processor to handle the computational requirements of the analysis.

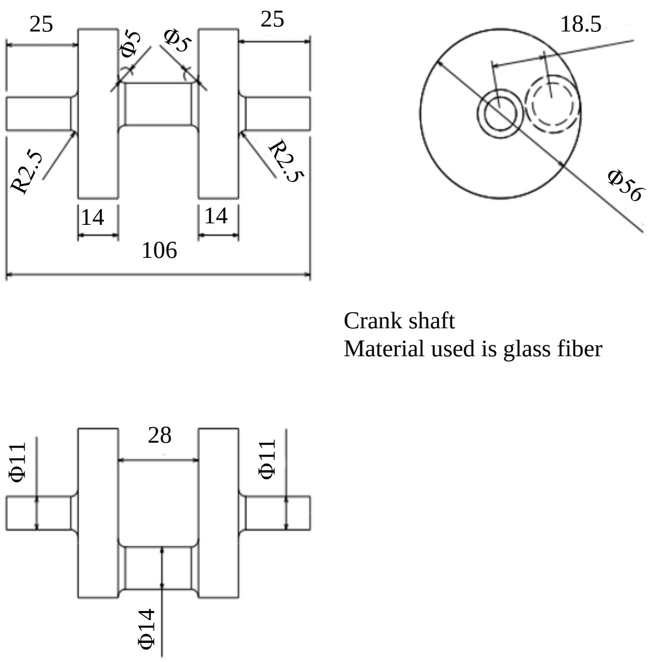

Figure 1. Dimensional characteristics of the crankshaft.

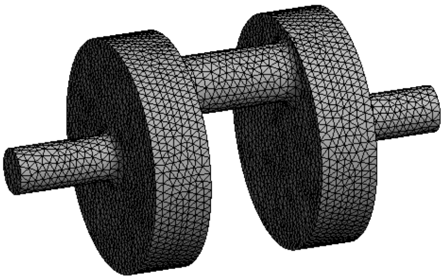

Figure 2. Meshing of crankshaft.

Figure 2 illustrates the finite element mesh generated for the crankshaft. The meshing process discretizes the crankshaft geometry into a dense network of interconnected elements capable of capturing stress gradients and deformation patterns with precision. A tetrahedral element type was selected due to its effectiveness in representing complex geometries and curved surfaces commonly found in crankshaft structures. The chosen element size of 3 mm provided an optimal balance between computational efficiency and analytical accuracy.

The final mesh comprised 44,499 nodes and 25,573 elements, ensuring adequate resolution in critical regions such as crank fillets, crankpins, and journal transitions—areas where stress concentrations typically arise. The refined mesh enabled the FEA model to replicate the crankshaft's structural response with a high degree of reliability, forming the backbone of subsequent stress, deformation, and fatigue evaluations.

This meshing framework established the numerical foundation needed to evaluate the influence of material substitution and guided the optimization effort to achieve a lightweight yet mechanically robust crankshaft.

RESULTS AND DISCUSSION

The finite element analysis conducted in the earlier stages of this investigation demonstrated that tetrahedral elements are particularly well-suited for modelling complex geometries such as the crankshaft. Their ability to conform to curved surfaces and intricate fillet regions ensures that stress concentrations and deformation gradients are captured with high accuracy. The mesh density employed—consisting of 44,499 nodes and 25,573 elements—played a crucial role in enhancing the fidelity of the simulation results. Such a finely discretized model allows for accurate representation of stress flow and structural response under load.

Figure 3a illustrates the boundary conditions applied to the steel crankshaft model, clearly depicting the regions where the gas load is imposed on the crankpin and where the supporting constraints are introduced. These boundary conditions replicate the crankshaft's actual loading environment during engine operation, ensuring that the simulation remains representative of real-world conditions.

The deformation results for the steel crankshaft are shown in Figure 3b. The maximum displacement recorded is only 0.01 mm, which is significantly low and indicative of the high stiffness associated with steel. The minimal deformation confirms that the crankshaft maintains structural integrity even under peak loading conditions, demonstrating its ability to withstand operational stresses without experiencing detrimental displacement.

Figure 3c presents the von Mises stress distribution for the steel iteration. The peak stress value of 55.39 MPa remains well below the material's yield strength, confirming that the crankshaft operates safely within its elastic region. The stress contours reveal expected concentration zones at fillets and crankpin transitions, highlighting areas of localized loading but confirming the adequacy of the existing steel design.

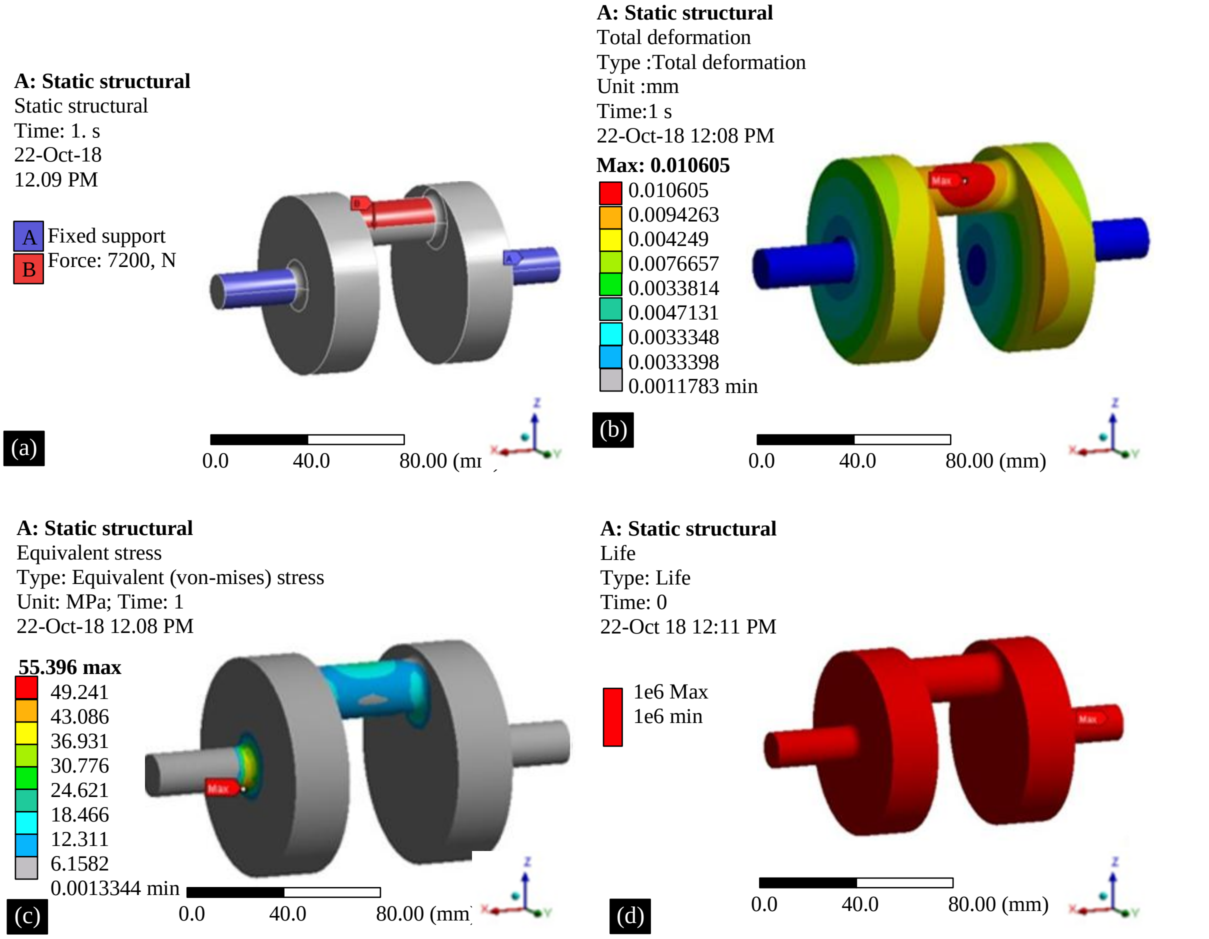

Figure 3. a: Applied boundary conditions highlight how forces and constraints are applied to the crankshaft. (b): Shows deformation under load, with a maximum of 0.01 mm observed in the crankshaft. (c): Displays von Mises stress distribution, with a maximum stress value of 55.39 MPa. **(**d): Fatigue life analysis indicates that the crankshaft can endure 1,000,000 cycles before failure.

Fatigue life predictions for the steel crankshaft are shown in Figure 4. The estimated fatigue life of approximately 1,000,000 cycles demonstrates substantial durability, indicating that the steel crankshaft is capable of withstanding long-term cyclic loading without crack initiation or propagation. This validates the robustness of the existing steel configuration.

The analysis was subsequently extended to evaluate the performance of carbon fiber as a material substitute. Figure 4a outlines the boundary condition setup for the carbon fiber iteration, ensuring that the applied loads and constraints remain consistent with the steel case, thus enabling an equitable comparison. The results depicted in Figure 4b reveal that the deformation increases significantly to 0.17 mm. Such a pronounced displacement reflects the lower stiffness of carbon fiber relative to steel and raises concerns regarding dimensional stability under dynamic operating conditions.

The von Mises stress contours for the carbon fiber crankshaft, illustrated in Figure 4c, show a maximum stress of 67.992 MPa. This value approaches or exceeds the permissible limits for the material, indicating that the carbon fiber crankshaft would be structurally inadequate under the same loading conditions. The stress distribution further demonstrates a lack of uniform load transfer compared to steel, which can lead to premature structural degradation.

Figure 4d presents the fatigue life estimation for the carbon fiber iteration, showing a predicted life of 991,000 cycles. Although marginally close to that of steel, this reduction, combined with higher deformation and excessive stress, highlights the inability of carbon fiber to serve as a viable replacement material for crankshaft applications. The combined evidence from deformation, stress analysis, and fatigue predictions confirms that carbon fiber lacks the stiffness and stress-handling capacity required for such a high-demand mechanical component.

Figure 5a presents the applied boundary conditions for the glass fiber crankshaft model. Similar to the earlier iterations performed for steel and carbon fiber, identical loading and constraint conditions were imposed to ensure a consistent basis for comparison. This standardized setup enables an accurate evaluation of how glass fiber responds under real engine-like operational stresses, allowing the material's structural behavior to be assessed without influence from external modelling variations.

The deformation results for the glass fiber crankshaft, illustrated in Figure 5b, indicate a maximum displacement of 0.16 mm. Although higher than that of steel (0.01 mm), this value remains lower than the deformation observed for carbon fiber (0.17 mm). The reduced deformation relative to carbon fiber suggests that glass fiber provides improved stiffness and dimensional stability, placing it as a structurally viable candidate for crankshaft applications where moderate flexibility can be tolerated without compromising functionality.

Figure 5c displays the von Mises stress distribution for the glass fiber iteration. The maximum stress recorded is 40.44 MPa, substantially lower than the peak stresses observed in both steel (55.39 MPa) and carbon fiber (67.99 MPa). This reduction in stress levels is highly favorable, indicating that the glass fiber configuration experiences less internal loading and thus offers improved operational safety and structural reliability. The stress contours also show a more uniform distribution, reflecting effective load transfer within the glass fiber composite matrix.

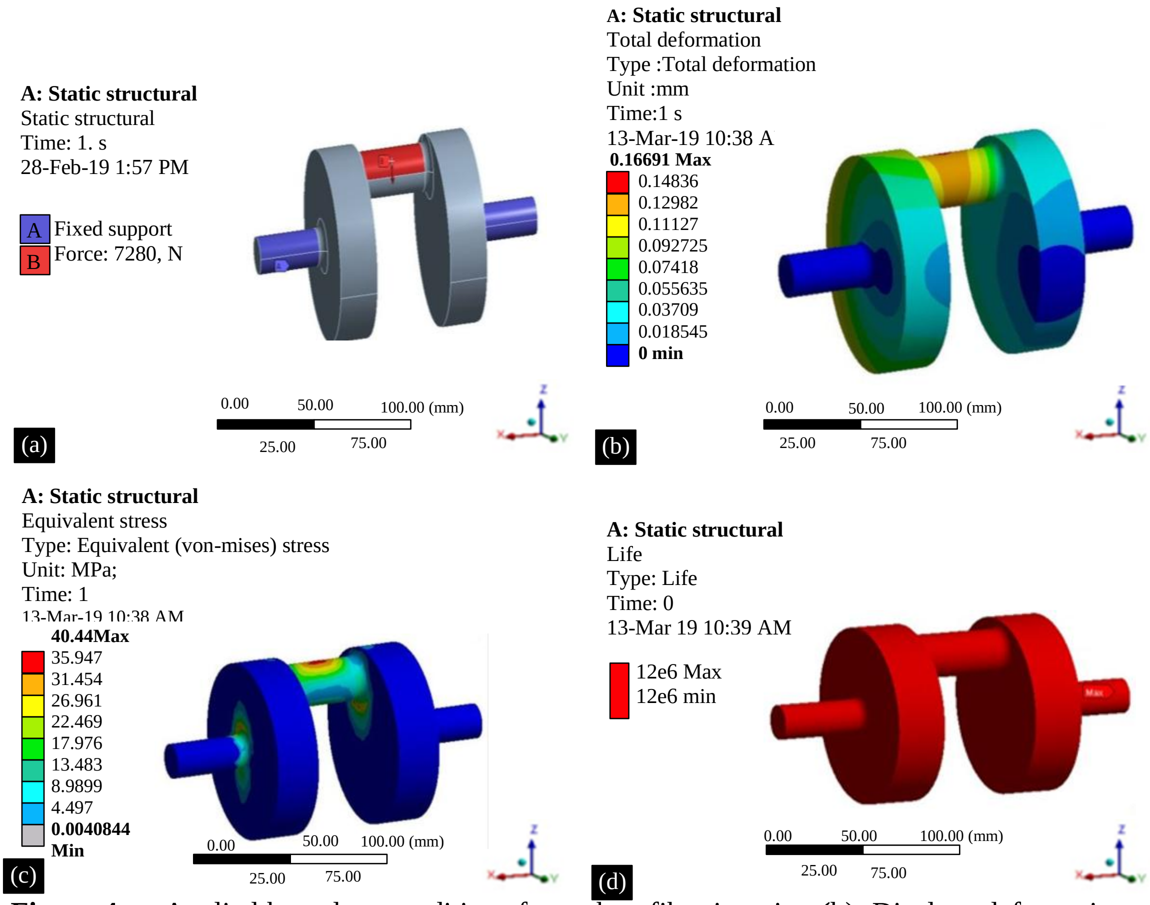

Figure 4. a: Applied boundary conditions for carbon fiber iteration **(**b): Displays deformation, which increases to 0.17 mm, unsuitable for design **(**c): von Mises stress rises to 67.992 MPa **(**d): Fatigue life decreases to 991,000 cycles.

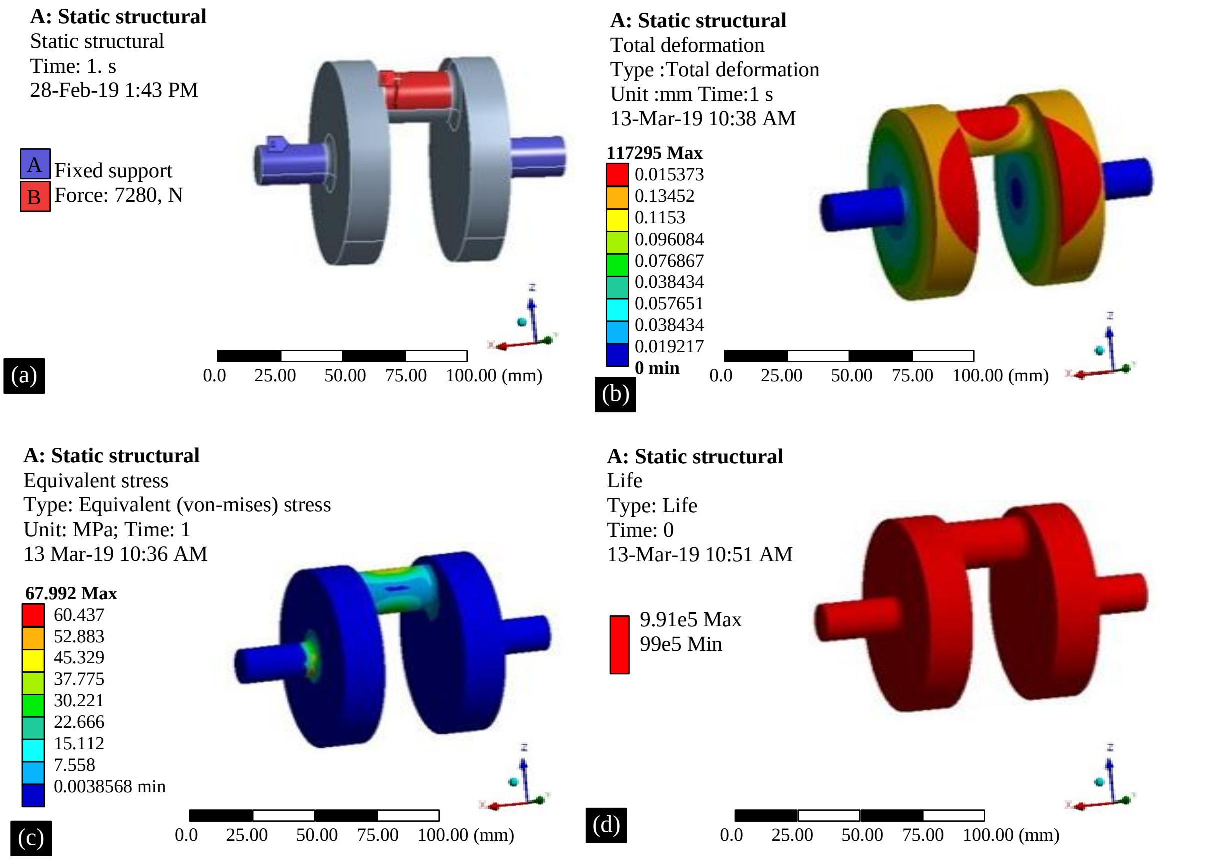

Figure 5. a: Applied boundary conditions for glass fiber iteration (b) Shows deformation of 0.16 mm, slightly higher than steel but permissible (c)von Mises stress reduces to 40.44 MPa, which is favorable **(**d)Fatigue life increases to 1,200,000 cycles, proving glass fiber as an optimized material.

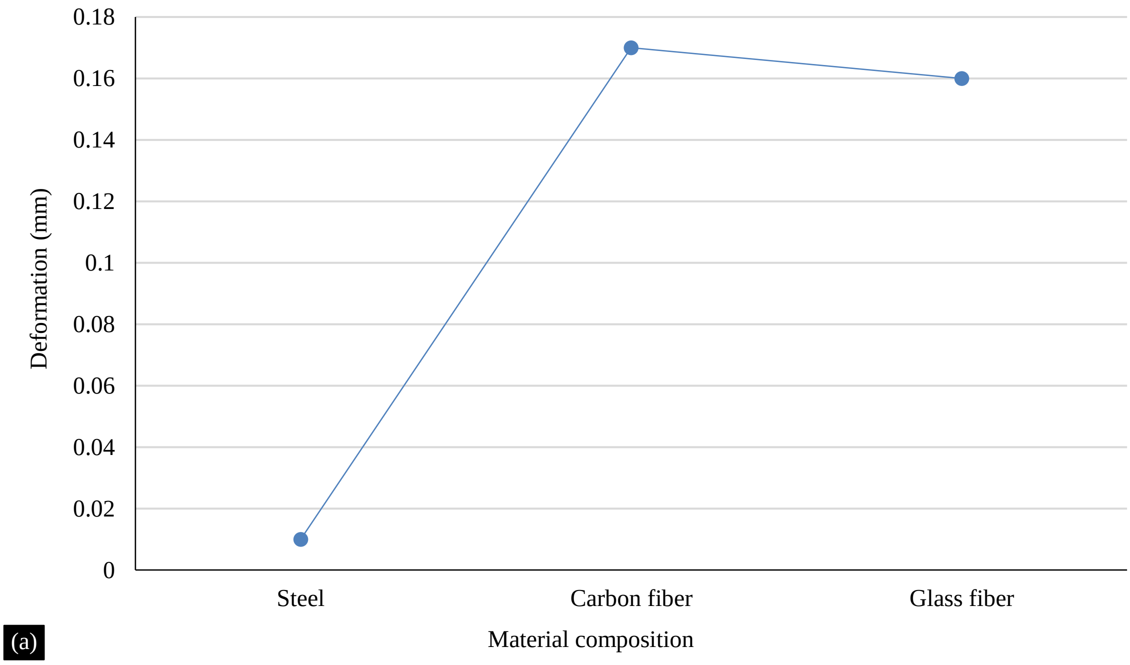

Figure 6. a: Compares deformation across materials: steel (0.01 mm), carbon fiber (0.17 mm), and glass fiber (0.16 mm).

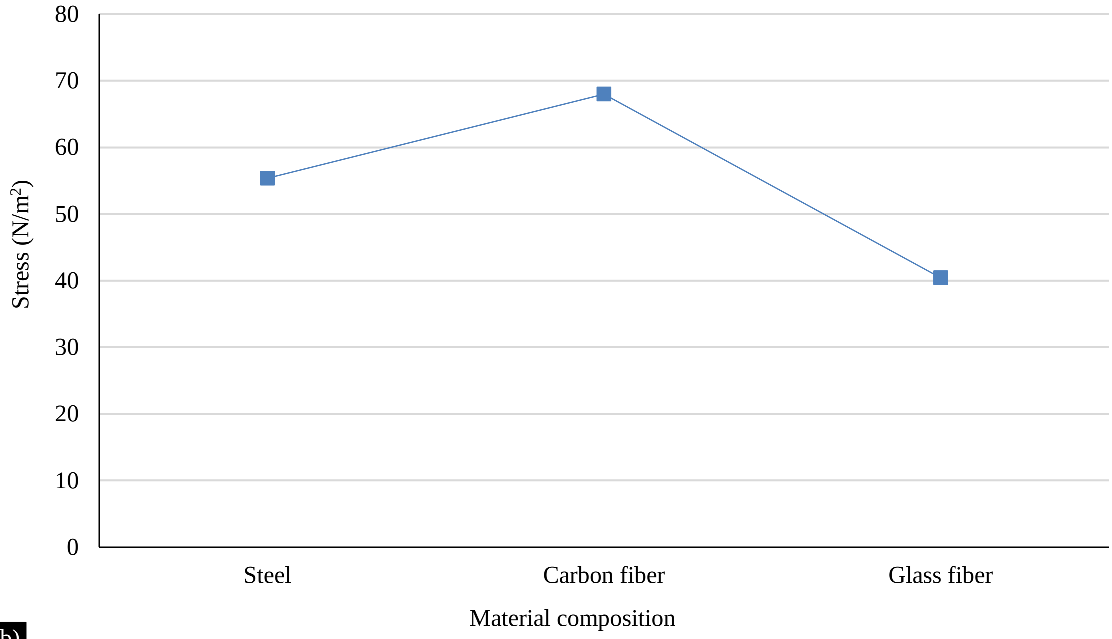

Figure 6. b: Shows von Mises stress comparison: steel (55.39 MPa), carbon fiber (67.992 MPa), and glass fiber (40.44 MPa).

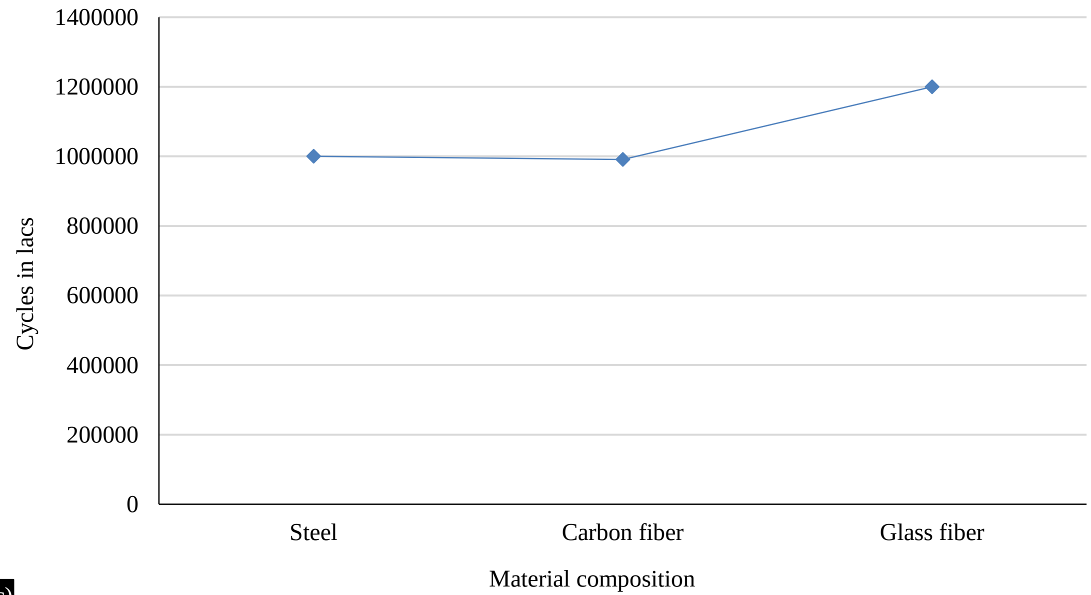

Figure 6. c: Compares fatigue life: steel (1,000,000 cycles), carbon fiber (991,000 cycles), and glass fiber (1,200,000 cycles).

The fatigue analysis results, shown in Figure 5d, further reinforce the suitability of glass fiber for crankshaft optimization. The predicted fatigue life of approximately 1,200,000 cycles surpasses both steel (1,000,000 cycles) and carbon fiber (991,000 cycles). This extended fatigue life highlights the superior durability of glass fiber under cyclic loading conditions and demonstrates its ability to sustain long-term operational demands without premature failure. The combination of low stress, moderate deformation, and enhanced fatigue life positions glass fiber as a particularly promising material for achieving significant weight reduction while maintaining or improving structural performance as shown in Figures 6a-6c. The test setup is also shown in Figure 7.

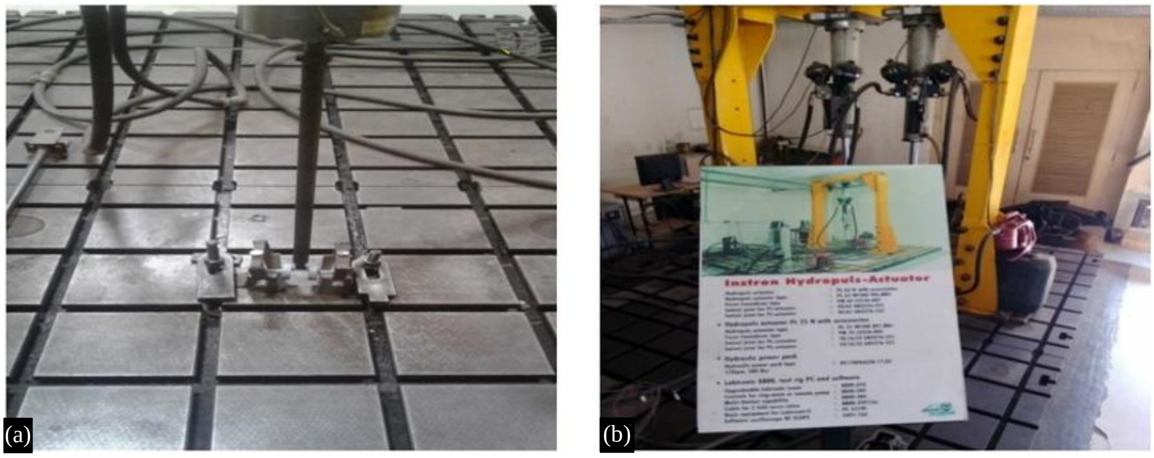

Figure 7. Test setup (a) clamping assembly and (b) Fatigue testing.

Taken together, these findings establish glass fiber as a reliable, high-performance alternative to traditional steel for crankshaft manufacturing, offering an optimal balance of stiffness, strength, fatigue resistance, and weight efficiency.

CONCLUSION

The experimental and numerical investigations carried out in this study demonstrate the strong potential of glass fiber as an effective lightweight alternative to steel for crankshaft applications. Fatigue testing performed at a loading frequency of 100 Hz revealed exceptional durability, with the glass fiber crankshaft completing 1,200,100 cycles without exhibiting any signs of crack initiation or structural degradation. This performance aligns closely with the finite element analysis (FEA) predictions, which also indicated a fatigue life exceeding 1,200,000 cycles. The close correspondence between experimental and numerical results confirms the reliability of the simulation methodology and validates the robustness of the glass fiber design.

One of the most significant findings of this study is the substantial weight reduction achieved through material substitution. The glass fiber crankshaft demonstrated an impressive 75.88% decrease in weight compared to the conventional steel crankshaft. This reduction directly enhances engine efficiency, reduces inertia, and contributes to improved fuel economy and overall performance in two-wheeler engines.

In terms of structural performance, the glass fiber crankshaft exhibited a 26.99% lower von Mises stress than its steel counterpart under identical loading conditions. This reduction in stress highlights the ability of the glass fiber composite to distribute loads more effectively, thereby improving structural integrity and reducing the likelihood of failure under operational stresses.

The fatigue life improvement is similarly noteworthy. FEA results revealed that the fatigue life of the glass fiber crankshaft surpasses that of steel by 16.66%, indicating superior endurance under prolonged cyclic loading. This enhancement, coupled with reduced stress levels and significant weight savings, underscores the suitability of glass fiber as a high-performance material for crankshaft optimization.

Overall, the combined experimental and numerical findings establish glass fiber as a highly durable, structurally reliable, and weight-efficient alternative to steel. The outcomes of this study open new avenues for the adoption of composite materials in critical engine components, offering a pathway toward lighter, more efficient, and high-performing automotive systems.

REFERENCES

1. Suganthini Rekha R, Nallusamy S, Vijayakumar R, Saravanan S. Modelling and analysis of crankshaft with metal matrix composites. Int J Appl Eng Res. 2015;10(62):1-5.

2. Pore EB, Kotkar DR. Modeling and analysis of aluminum alloy crankshaft for optimization of weight using FEA. Int J Tech Res Appl. 2016;4(2):156-162.
3. Gopal G, Suresh Kumar L, VijayaBahskar Reddy K, Uma Maheshwara Rao M, Srinivasulu G. Analysis of piston, connecting rod, and crankshaft assembly. Mater Today Proc. 2017;4:7810-7819.
4. Witek L, Sikora M, Stachowicz F, Trzepiecinski T. Stress and failure analysis of the crankshaft of diesel engine. Eng Fail Anal. 2017. doi:10.1016/j.engfailanal.2017.06.001.
5. Witek L, Stachowicz F, Załęski A. Failure investigation of the crankshaft of diesel engine. Struct Integr Procedia. 2016;1:1-7.
6. Jamalkhani Khameneh M, Azadi M. Evaluation of high-cycle bending fatigue and fracture behaviors in EN-GJS700-2 ductile cast iron of crankshafts. Eng Fail Anal. 2018;85:189-200.
7. Zhenpeng H, Wenqin G, Weisong X, Junhong Z, Guichang Z, Hong Z. NVH and reliability analyses of the engine with different interaction models between the crankshaft and bearing. Appl Acoust. 2016;101:185-200.
8. Satishkumar S, Kannan M. Structural, thermal, and thermo-mechanical analysis of four-stroke petrol engine piston using CAE tools. ICICET. 2018:978-93-5291-751-8.
9. Fonte M, Infante V, Freitas M, Reis L. Failure mode analysis of two diesel engine crankshafts. Procedia Struct Integr. 2016;1:313-318.
10. Senthilkumar M, Ragunathan S, Suresh M, Srinivashan VR. A study of crankpin failure in IC engine. Mech Eng Int J. 2014;1(3):1-7.
11. Bagde BJ, Raut LP. Finite element structural and fatigue analysis of single-cylinder engine crankshaft. Int J Eng Res Technol. 2013;2(7):1-6.
12. Thejasree P, Dileep Kumar G, LeelaPrasanna Lakshmi S. Modelling and analysis of crankshaft for passenger car using FEA. Mater Today Proc. 2017;4:11292-11299.
13. Kahate C, Keche A. Failure analysis of crankshaft using finite element approach. Int J Eng Appl Sci. 2016;3(4):1-6.
14. Patil S, Pawar SR. Static analysis of composite crankshaft of single-cylinder petrol engine using ANSYS software. J Emerg Technol Innov Res. 2018;5(6):1-7.
15. Mathapati NC, Dhamejani CL. FEA of a crankshaft in crank-pin web fillet region for improving fatigue life. Int J Innov Eng Res Technol. 2015;2(6):1-5.
16. Devara AK. Finite element analysis of crankshaft. Natl Conf Adv Mech Eng. Manipal; 2011.
17. Kolhe SK, Ghare P, Chaudhari A. Diesel engine crankshaft high-cycle fatigue life estimation and improvement through FEA. Int J Eng Res Technol. 2016;1(1):1-6.
18. Ramani J, Ramani H, Suhagiya S. FE-analysis of crankshaft of IC engine for increasing the breathing capacity. Int J Eng Res Appl. 2013;3(2):1-6.
19. Kakade P, Pasarkar MD. Analyzing and identifying various approaches for crankshaft failures. J Multidiscip Eng Sci Technol. 2015;2(2):1-5.
20. Kumbhar AU, Kumbhar SR, Diwate VS. Design and failure analysis of four-stroke six-cylinder diesel engine crankshaft. Tech Res Organ India. 2016;3(6):1-6.
21. Naik SA. Failure analysis of crankshaft by finite element method: A review. Int J Eng Trends Technol. 2015;19(5):1-5.
22. Marpudi VS, Mehra RS. Fatigue failure analysis of an automotive crankshaft and its behavior under different operating loads. Int J Eng Res Technol. 2014;3(1):1-6.
23. Ayrilmis N, Kanat G, Yildiz Avsar E, Palanisamy S, Ashori A. Utilizing waste manhole covers and fibreboard as reinforcing fillers for thermoplastic composites. J Reinf Plast Compos. 2025;44(17-18):1108-1118. doi:10.1177/07316844241238507.
24. Almeshaal M, Palanisamy S, Murugesan TM, Palaniappan M, Santulli C. Physico-chemical characterization of Grewia monticola Sond (GMS) fibers for prospective application in biocomposites. J Nat Fibers. 2022;19(17):15276-15290. doi:10.1080/15440478.2022.2123076.
25. Palanisamy S, Mayandi K, Palaniappan M, Alavudeen A, Rajini N, Vannucchi de Camargo F, et al. Mechanical properties of Phormium tenax reinforced natural rubber composites. Fibers. 2021;9(2):11. doi:10.3390/fib9020011.

26. Rajkumar R, Kayambu A, Palanisamy S, Ayrilmis N. Mechanical properties of epoxy composites reinforced with Areca catechu fibers containing silicon carbide. BioResources. 2024;19(2):2353-2370. doi:10.15376/biores.19.2.2353-2370.
27. Palanisamy S, Mayandi K, Dharmalingam S, Rajini N, Santulli C, Mohammad F, et al. Tensile properties and fracture morphology of Acacia caesia bark fibers treated with different alkali concentrations. J Nat Fibers. 2022;19(15):11258-11269. doi:10.1080/15440478.2021.2022562.

